Introduction

Parkinson's disease (PD) is the most common neurodegenerative movement disorder that causes progressive motor symptoms mainly due to gradual loss of dopaminergic neurons in the substantia nigra pars compacta (de Lau *et al.,* 2006). Treatments that provide neuroprotection and/or disease-modifying effects remain an unmet clinical need because currently available dopamine replacement therapies only partially improve the symptoms (Meisnner *et al.,* 2011).

Though PD is typically sporadic in origin, identification of genes responsible for familial PD have provided clues to understand the pathogenesis of the more common, sporadic form of PD (Moore *et al.,* 2008). Parkin, PINK1 and DJ-1 are causative genes of autosomal recessive PD, in which clinical phenotype is often indistinguishable from early-onset idiopathic PD (Kitada *et al.,* 1998; Valente *et al.,* 2004; Bonifati *et al.,* 2003). Identification of these genes have promoted generation of gene-modified models to investigate the pathomechanisms of the disease (Shulman *et al.,* 2011).

Recent studies have revealed that these genes share, at least in part, a common pathway in mitochondria quality control and protein quality control. Genetic studies using Parkin and PINK1 knockout *Drosophila* indicated that PINK1 acts upstream of Parkin (Clark *et al.,* 2006; Park *et al.,* 2006; Yang *et al.,* 2006). Further studies elucidated that Parkin and PINK1 share a common mitochondrial quality control pathway conserved in mammalian cells (Narendra *et al.,* 2011; Matsui, Gavinio and Asano *et al.,* 2013). Meanwhile, it is still controversial whether DJ-1 works in association with PINK1/Parkin pathway (Yang *et al*., 2006; Exner *et al.,* 2007; Hao *et al.,* 2010; Thomas *et al*., 2011). Although several previous studies suggested that Parkin and/or PINK1 interact with DJ-1 to promote protein degradation (Olzmann *et al.,* 2007; Xiong *et al.,* 2009), the precise genetic and functional relationships between these genes remain elusive.

Genetic mammalian models of autosomal recessive PD, such as Parkin-, PINK1- and DJ-1-knockout mice, have failed to recapitulate the hallmark features of PD, especially the progressive loss of nigral dopaminergic neurons (Moore *et al.,* 2008). Furthermore, aged triple knockout mice lacking Parkin, DJ-1, and PINK1 do not exhibit PD-related phenotypes (Kitada *et al.,* 2009). These observations raise the possibility of functional redundancy among mice genes and suggest the limitation of gene-modified mice model to clarify the relationship among these genes (Shulman *et al.,* 2011). A novel model using higher vertebrates would be helpful to further reveal their functional association.

Here we established *DJ-1 -/-* DT40 cells and examined their phenotype to evaluate whether DT40 cells could be used as a relevant model of PD. DT40 is an avian leukosis virus-induced chicken B cell line with an exceptionally high ratio of targeted to random DNA integration of a transfected genomic DNA fragment to its homologous genomic locus (Buerstedde and Takeda., 1991). This feature enables efficient targeted gene disruption in vertebrate cells without generating a knockout animal model. We report that *DJ-1 -/-* DT40 cells recapitulate multiple phenotypes compatible to those of DJ-1 deficient mammalian cells and that mitochondrial membrane potential and morphology are available as a readout of phenotype analysis in DT40 cells.

Results

Generation of DJ-1 -/- DT40 Cells — We disrupted two *DJ-1* alleles by sequentially transfecting the two targeting constructs (Fig. 1A) carrying puromycin or histidinol resistance gene into DT40 cells (Iiizumi *et al.*, 2006, Kohzaki *et al.*, 2010). Disruption of both alleles was confirmed by genomic Southern blotting (Fig. 1B). Absence of detectable mRNA or protein was confirmed by RT-PCR using primers designed to flank drug-resistance gene (Fig. 1C) and western blotting (Fig. 1D). In the following phenotype analyses, experiments were repeated independently three times using one representative DJ-1 -/- clone after having confirmed by a preliminary experiment that two or three different DJ-1 -/- clones exhibit the same phenotype.

Increased vulnerability to oxidative stress in DJ-1 -/- DT40 cells — DJ-1 was originally identified as an oncogene and was found to be the causative gene of autosomal recessive Parkinson's disease, PARK7 (Nagakubo *et al.*, 1997, Bonifati *et al.*, 2003). Although DJ-1 has been suggested to have multiple possible functions, a consistent finding is that DJ-1 protects against oxidative stress *in vitro* and *in vivo* (Cookson, 2010). Therefore, we first investigated whether this was recapitulated in DT40 cells. We treated cells with H_2O_2 and determined intracellular accumulation of ROS by flow cytometric analysis with 5-(and-6)-carboxy-2',7'-dichlorodihydrofluorescein diacetate (carboxy-H_2DCFDA). *DJ-1* -/- DT40 cells showed significantly increased accumulation of intracellular ROS compared to wild type cells (Fig. 2A). To examine vulnerability of *DJ-1* -/- DT40 cells to oxidative stress, we analyzed H_2O_2-induced cell death by labeling the cells with Annexin-V and propidium iodide. At 24 hours after H_2O_2 treatment, we measured the ratio of viable cells, early-apoptotic cells, and late-apoptotic and necrotic cells by flow cytometric analysis. We found that the ratio of viable cells was significantly lower and that early-apoptotic and late-apoptotic and necrotic cells were significantly higher in *DJ-1* -/- cells than in wild type cells (Fig. 2B, 2C). These results were compatible with the notion that DJ-1 has physiological antioxidant property in DT40 cells.

Decreased mitochondrial membrane potential in DJ-1 -/- DT40 cells — Mitochondrial dysfunction has long been implicated in the etiopathogenesis of PD (Imai *et al.*, 2011). Indeed, DJ-1-deficient mammalian cells show mitochondrial dysfunction (Krebiehl *et al.*, 2010). To analyze whether loss of DJ-1 resulted in mitochondrial dysfunction in DT40 cells, we evaluated mitochondrial membrane potential (MMP) using the following two MMP-dependent dyes, MitoTracker Red CMXRos and tetramethylrhodamine ethyl ester (TMRE). The staining with the former reagent showed a decrease of MMP in DJ-1 -/- DT40cells, as indicated by lower levels of staining in the mutant cells compared to wild type DT40 cells (Fig. 3A). We confirmed this result by detecting the intensity of TMRE staining, a quantitative indicator of membrane potential, by flow cytometry. The MMP of *DJ-1* -/- DT40 cells was significantly decreased compared to wild type cells (Fig. 3B, 3C). To exclude the possibility that the decreased staining with these dyes was caused by a decrease in the number of mitochondria, we stained the cells with MitoTracker Green, which is a MMP-independent dye. The intensity of MitoTracker Green signals did not differ between wild type and *DJ-1* -/- cells. This indicated that the reduced staining with MitoTracker Red CMXRos or TMRE was not due to decrease in the number of mitochondria in *DJ-1* -/- cells (Fig. 3D). Overall,

these results suggested that loss of DJ-1 in DT40 cells resulted in decreased mitochondrial membrane potential.

Fragmented mitochondria in DJ-1 -/- DT40 cells — Recent studies have consistently demonstrated that DJ-1-deficient mammalian cells exhibit mitochondrial fragmentation (Krebiehl *et al.,* 2010;Irrcher *et al.*, 2010). To confirm the reproducibility of this phenotype in *DJ-1 -/-* DT40 cells, we immunostained mitochondria with Tom20, a mitochondrial outer membrane specific protein, and imaged by laser confocal microscope (Fig. 4A). We determined the average size of mitochondria using Spot Detector software by analyzing the size of each spot surrounded by Tom20-positive signal and the number of the spots per cell. Remarkably, in *DJ-1 -/-* DT40 cells, the average size of these spots was significantly decreased (Fig. 4B) and the number of these spots per cell was significantly increased (Fig. 4C) compared to wild type DT40 cells.

Discussion

In the present study, we generated DJ-1 deficient DT40 cells, which exhibited vulnerability to oxidative stress, mitochondrial dysfunction and mitochondrial fragmentation.

We utilized DT40, a lymphocyte cell line, as a novel PD cellular model. The rationale for our approach is that Parkin, PINK1 and DJ-1 are highly conserved across species and are expressed in lymphocytes. Moreover, analysis of lymphocytes would contribute to understanding the pathomechanism of PD. This is evidenced by subclinical PD-related phenotypes in lymphocytes or lymphoblasts of PD patients. Mitochondrial dysfunction and increased oxidative stress were observed in lymphocytes of PD patients (Müftüoglu *et al*., 2004; Prigione *et al*., 2009). Lymphoblasts established from a PD patient with DJ-1 mutation exhibited abnormal mitochondrial fragmentation (Irrcher *et al*., 2010). These subclinical phenotypes are consistent with the phenotype of DJ-1-deficient DT40 cells. These lines of evidence support the recent concept of PD as a systemic disorder (Imai *et al.,* 2011) and demonstratesthe validity of our approach. Although the effect of DJ-1 loss in DT40 cells on ROS accumulation and mitochondrial membrane potential were relatively small compared to previous studies, we speculate that this was because of the highly rapid turnover of DT40 cells. Furthermore, although the mitochondrial morphology is relatively fragmented in wild type DT40 cells compared to those typically observed in adherent culture cell lines, the difference in the quantitated Tom20-positive area indicated that loss of *DJ-1* led to further mitochondrial fragmentation in DT40 cells.

The advantage of this approach compared to the currently-available cellular models including induced pluripotent stem cells-derived lines from patients, mouse embryonic fibroblasts from knockout mice and RNAi approaches, are the efficacy and consistency in generating and analyzing the effect of multiple gene disruption. These advantages rely on the following multiple unique characteristics of this cell line. Firstly, DT40 cell line exhibits the extraordinary high ratio of targeted to random DNA integration (Buerstedde and Takeda, 1991). This ensures highly efficient multiple targeted gene disruption in a single cell using seven different selection markers, which can be recycled by the cre/loxP (Winding *et al.,* 2001; Arakawa *et al*., 2001). Secondly, although RNAi technology has been widely used in mammalian cell lines for targeted knockdown, the residual mRNA is always

problematic for interpretation of the resulting phenotype (Neumann *et al.*, 2010). Genetically engineered knockout of DT40 helps overcome this problem. The fact that wild type and gene-disrupted DT40 cells have completely identical genetic background also contributes to increase consistency in phenotype analysis. Moreover, DT40 cells have a short doubling time (~8h) and are genetically stable even after repeated passages compared to mammalian cells including mouse embryonic fibroblasts. These also help increase efficiency and consistency in phenotype analysis.

All these features make DT40 cell line attractive for analyzing effects of gene disruption as well as functional relationships among multiple genes. These advantages of DT40 cell lines have been previously taken to analyze the functions of B cell antigen receptor signaling, histone gene function, RNA processing, DNA repair, cell cycle, calcium signaling and autophagy (Winding *et al*., 2001; Alers *et al*., 2011). As accumulating evidence suggests the primary role of mitochondrial dysfunction in the pathomechanism of PD (Schapira, 2012), it is crucial to evaluate mitochondria function in PD models. We showed that mitochondrial membrane potential and morphology are available as a readout of phenotypic analysis in DT40 cells.

Generation and functional analyses of double- or triple- knockout DT40 cell model of Parkin, PINK1 and DJ-1 will help further reveal the functional association among these genes in the maintenance of mitochondria as well as in the pathophysiology of PD. Furthermore, elucidating the pathomechanism of PD using DT40 lymphocyte line could lead to the development of novel tools to utilize patients' lymphocytes as noninvasive diagnostic or therapeutic biomarkers. This approach also has a great potential for developing high-throughput assays for drug screening using patient-derived lymphocytes.

References

Alers, S., Löffler, A.S., Paasch, F., Dieterle, A.M., Keppeler, H., Lauber, K., Campbell, D.G., Fehrenbacher, B., Schaller, M., Wesselborg, S. and Stork, B., 2011. Atg13 and FIP200 act independently of Ulk1 and Ulk2 in autophagy induction. Autophagy 7, 1424-33.

Arakawa, H., Lodygin, D. and Buerstedde, J. M., 2001. Mutant loxP vectors for selectable marker recycle and conditional knock-outs. BMC Biotechnol. 1, 7.

Bonifati, V., Rizzu, P., van Baren, M. J., Schaap, O., Breedveld, G. J., Krieger, E., Dekker, M. C. J., Squitieri, F., Ibanez, P., Joosse, M., van Dongen, J. W., Vanacore, N., van Swieten, J. C., Brice, A., Meco, G., van Duijn, C. M., Oostra, B. A. and Heutink, P., 2003. Mutations in the DJ-1 gene associated with autosomal recessive early-onset parkinsonism. Science 299, 256–259

Buerstedde, J. M. and Takeda, S., 1991. Increased ratio of targeted to random integration after transfection of chicken B cell lines. Cell 67, 179–188.

Clark, I. E., Dodson, M. W., Jiang, C., Cao, J. H., Huh, J. R., Seol, J. H., Yoo, S. J., Hay, B. A. and Guo, M., 2006. Drosophila pink1 is required for mitochondrial function and interacts genetically with parkin. Nature 441, 1162–1166.

Cookson, M. R., 2010. DJ-1, PINK1, and their effects on mitochondrial pathways. Mov. Disord. 25 Suppl 1, S44–48.

de Lau, L. M. L. and Breteler, M. M. B., 2006. Epidemiology of Parkinson's disease. Lancet Neurol 5, 525–535.

Exner, N., Treske, B., Paquet, D., Holmström, K., Schiesling, C., Gispert, S., Carballo-Carbajal, I., Berg, D., Hoepken, H.-H., Gasser, T., Krüger, R., Winklhofer, K. F., Vogel, F., Reichert, A. S., Auburger, G., Kahle, P. J., Schmid, B. and Haass, C., 2007. Loss-of-function of human PINK1 results in mitochondrial pathology and can be rescued by parkin. J. Neurosci. 27, 12413–12418.

Hao, L.-Y., Giasson, B. I. and Bonini, N. M., 2010. DJ-1 is critical for mitochondrial function and rescues PINK1 loss of function. Proc. Natl. Acad. Sci. U.S.A. 107, 9747–9752.

Iiizumi, S., Nomura, Y., So, S., Uegaki, K., Aoki, K., Shibahara, K., Adachi, N. and Koyama, H., 2006. Simple one-week method to construct gene-targeting vectors: application to production of human knockout cell lines. BioTechniques 41, 311–316.

Imai, Y. and Lu, B., 2011. Mitochondrial dynamics and mitophagy in Parkinson's disease: disordered cellular power plant becomes a big deal in a major movement disorder. Curr. Opin. Neurobiol. 21, 935–941.

Irrcher, I., Aleyasin, H., Seifert, E. L., Hewitt, S. J., Chhabra, S., Phillips, M., Lutz, A. K., Rousseaux, M. W. C., Bevilacqua, L., Jahani-Asl, A., Callaghan, S., MacLaurin, J. G., Winklhofer, K. F., Rizzu, P., Rippstein, P., Kim, R. H., Chen, C. X., Fon, E. A., Slack, R. S., Harper, M. E., McBride, H. M., Mak, T. W. and Park, D. S., 2010. Loss of the Parkinson's disease-linked gene DJ-1 perturbs mitochondrial dynamics. Hum. Mol. Genet. 19, 3734–3746.

Kitada, T., Asakawa, S., Hattori, N., Matsumine, H., Yamamura, Y., Minoshima, S., Yokochi, M., Mizuno, Y. and Shimizu, N., 1998. Mutations in the parkin gene cause autosomal recessive juvenile parkinsonism. Nature 392, 605–608.

Kitada, T., Tong, Y., Gautier, C. A. and Shen, J., 2009. Absence of nigral degeneration in aged parkin/DJ-1/PINK1 triple knockout mice. J. Neurochem. 111, 696–702.

Kohzaki, M., Nishihara, K., Hirota, K., Sonoda, E., Yoshimura, M., Ekino, S., Butler, J. E., Watanabe, M., Halazonetis, T. D. and Takeda, S., 2010. DNA polymerases nu and theta are required for efficient immunoglobulin V gene diversification in chicken. J. Cell Biol. 189, 1117–1127.

Krebiehl, G., Ruckerbauer, S., Burbulla, L. F., Kieper, N., Maurer, B., Waak, J., Wolburg, H., Gizatullina, Z., Gellerich, F. N., Woitalla, D., Riess, O., Kahle, P. J., Proikas-Cezanne, T. and Krüger, R., 2010. Basal autophagy and impaired mitochondrial dynamics due to loss of Parkinson's disease-associated protein DJ-1. PLoS ONE 5, e9367.

Matsui H., Gavinio R., Asano T., Uemura N., Ito H., Taniguchi Y., Kobayashi Y., Maki T., Shen J., Takeda S., Uemura K., Yamakado H., Takahashi R., 2013. PINK1 and Parkin complementarily protect dopaminergic neurons in vertebrates.Hum Mol Genet. 22, 2423-34.

Meissner, W. G., Frasier, M., Gasser, T., Goetz, C. G., Lozano, A., Piccini, P., Obeso, J. A., Rascol, O., Schapira,

A., Voon, V., Weiner, D. M., Tison, F. and Bezard, E., 2011. Priorities in Parkinson's disease research. Nat Rev Drug Discov 10, 377–393.
Moore, D. J. and Dawson, T. M., 2008. Value of genetic models in understanding the cause and mechanisms of Parkinson's disease. Curr Neurol Neurosci Rep 8, 288–296
Müftüoglu, M., Elibol, B., Dalmizrak, O., Ercan, A., Kulaksiz, G., Ogüs, H., Dalkara, T. and Ozer, N., 2004. Mitochondrial complex I and IV activities in leukocytes from patients with parkin mutations. Mov. Disord. 19, 544–548.
Nagakubo, D., Taira, T., Kitaura, H., Ikeda, M., Tamai, K., Iguchi-Ariga, S. M. and Ariga, H., 1997. DJ-1, a novel oncogene which transforms mouse NIH3T3 cells in cooperation with ras. Biochem. Biophys. Res. Commun. 231, 509–513.
Narendra, D. P. and Youle, R. J., 2011. Targeting mitochondrial dysfunction: role for PINK1 and Parkin in mitochondrial quality control. Antioxid. Redox Signal. 14, 1929–1938.
Neumann, B., Walter, T., Hériché, J.-K., Bulkescher, J., Erfle, H., Conrad, C., Rogers, P., Poser, I., Held, M., Liebel, U., Cetin, C., Sieckmann, F., Pau, G., Kabbe, R., Wünsche, A., Satagopam, V., Schmitz, M. H. A., Chapuis, C., Gerlich, D. W., Schneider, R., Eils, R., Huber, W., Peters, J.-M., Hyman, A. A., Durbin, R., Pepperkok, R. and Ellenberg, J., 2010. Phenotypic profiling of the human genome by time-lapse microscopy reveals cell division genes. Nature 464, 721–727
Olzmann, J. A., Li, L., Chudaev, M. V., Chen, J., Perez, F. A., Palmiter, R. D. and Chin, L.-S., 2007. Parkin-mediated K63-linked polyubiquitination targets misfolded DJ-1 to aggresomes via binding to HDAC6. J. Cell Biol. 178, 1025–1038.
Park, J., Lee, S. B., Lee, S., Kim, Y., Song, S., Kim, S., Bae, E., Kim, J., Shong, M., Kim, J.-M. and Chung, J., 2006. Mitochondrial dysfunction in Drosophila PINK1 mutants is complemented by parkin. Nature 441, 1157–1161.
Prigione, A., Isaias, I. U., Galbussera, A., Brighina, L., Begni, B., Andreoni, S., Pezzoli, G., Antonini, A. and Ferrarese, C., 2009. Increased oxidative stress in lymphocytes from untreated Parkinson's disease patients. Parkinsonism Relat. Disord. 15, 327–328.
Schapira, A. H. V., 2012. Mitochondrial diseases. Lancet 379, 1825–1834.
Shulman, J. M., De Jager, P. L. and Feany, M. B., 2011. Parkinson's disease: genetics and pathogenesis. Annu Rev Pathol 6, 193–222.
Thomas, K. J., McCoy, M. K., Blackinton, J., Beilina, A., van der Brug, M., Sandebring, A., Miller, D., Maric, D., Cedazo-Minguez, A. and Cookson, M. R., 2011. DJ-1 acts in parallel to the PINK1/parkin pathway to control mitochondrial function and autophagy. Hum. Mol. Genet. 20, 40–50.
Valente, E. M., Abou-Sleiman, P. M., Caputo, V., Muqit, M. M. K., Harvey, K., Gispert, S., Ali, Z., Del Turco, D., Bentivoglio, A. R., Healy, D. G., Albanese, A., Nussbaum, R., González-Maldonado, R., Deller, T., Salvi, S., Cortelli, P., Gilks, W. P., Latchman, D. S., Harvey, R. J., Dallapiccola, B., Auburger, G. and Wood, N. W., 2004.

Hereditary early-onset Parkinson's disease caused by mutations in PINK1. Science 304, 1158–1160.
Winding, P. and Berchtold, M. W., 2001. The chicken B cell line DT40: a novel tool for gene disruption experiments. J. Immunol. Methods 249, 1–16.
Xiong, H., Wang, D., Chen, L., Choo, Y. S., Ma, H., Tang, C., Xia, K., Jiang, W., Ronai, Z., Zhuang, X. and Zhang, Z., 2009. Parkin, PINK1, and DJ-1 form a ubiquitin E3 ligase complex promoting unfolded protein degradation. J. Clin. Invest. 119, 650–660.
Yang, Y., Gehrke, S., Imai, Y., Huang, Z., Ouyang, Y., Wang, J.-W., Yang, L., Beal, M. F., Vogel, H. and Lu, B., 2006. Mitochondrial pathology and muscle and dopaminergic neuron degeneration caused by inactivation of Drosophila Pink1 is rescued by Parkin. Proc. Natl. Acad. Sci. U.S.A. 103, 10793–10798.

Figure legends

FIGURE 1. Targeted disruption of DJ-1 in DT40 cells. A. Schematic representation of the chicken *DJ-1* locus and the gene-targeting constructs. Black squares indicate exon 2-7. The restriction enzyme sites and the probe used for genomic Southern blot analysis are shown. B. Southern blot analysis of BglII-digested genomic DNA from wild type, *DJ-1 +/-*, and *DJ-1 -/-* DT40 cells. C. Representative RT-PCR analysis of wild type and *DJ-1 -/-* cells. The forward primer was designed in exon 3, and the reverse primer was designed in exon 7. The expected length of amplicon from wild-type DT40 cells is 460 bp. No band corresponding to DJ-1 was observed in DJ-1 knockout cells. D. Western blot analysis of whole cell lysate from wild type and *DJ-1 -/-* DT40 cells. Blots were probed with anti-DJ-1 polyclonal antibody and anti-GAPDH polyclonal antibody. No band corresponding to DJ-1 was observed.

FIGURE 2. Increased vulnerability to oxidative stress in *DJ-1 -/-* DT40 cells. A. Flow cytometric analysis of intracellular ROS. Wild type or *DJ-1 -/-* DT40 cells were treated with 10uM H_2O_2 for 24 hours and stained with carboxy-H_2DCFDA, a ROS indicator. The fluorescence intensity was measured by flow cytometry. The amount of intracellular ROS after H_2O_2 treatment was significantly greater in *DJ-1 -/-* cells. Error bars indicate mean ± SEM values from three independent experiments. *P<0.05, N.S.; not significant by Bonferroni multiple comparison test. B. Representative flow cytometric analysis of cell viability after H_2O_2 treatment. Wild type or *DJ-1 -/-* DT40 cells were treated with 10 μM H_2O_2 for 24 hours and stained with Annexin-V (AV) and propium iodide (PI). Lower right quadrant (AV positive and PI negative) corresponds to early-apoptotic cells, and upper right quadrant (AV and PI doublepositive) corresponds to late-apoptotic and necrotic cells. Cells not stained with AV and PI (lower left quadrant) are viable cells. C. Quantification of viable, early-apoptotic, and late-apoptotic and necrotic cells after treatment with 10 μM H_2O_2 for 24 hours. The percentage of the cells in lower left (LL), lower right (LR) or upper right (UR) quadrant shown in figure 2B were quantified and were analyzed by Bonferroni multiple comparison test. Error bars indicate mean ± SEM values from three independent experiments. *P<0.05, N.S.; not significant.

FIGURE 3. Decreased mitochondrial membrane potential in *DJ-1 -/-* DT40 cells. A. Representative imaging of wild type and *DJ-1 -/-* DT40 cells stained with MitoTracker Red CMXRos. *DJ-1 -/-* cells had lower staining intensity of mitochondria than wild-type cells. CCCP treatment was performed as a positive control. B. Representative flow cytometric analysis of TMRE staining intensity. C. Quantification of TMRE staining. *DJ-1 -/-* cells had significantly lower TMRE staining. Three independent experiments were performed and analyzed by unpaired *t*-test. Error bars indicate mean ± SEM values. *P<0.01. D. Quantification of MitoTracker GreenFM staining from flow cytometric analysis. Three independent experiments were performed and analyzed by unpaired *t*-test. Error bars indicate mean ± SEM values. N.S.; not significant.

FIGURE 4. Fragmented mitochondria in *DJ-1 -/-* DT40 cells. A. Representative imaging of wild type and *DJ-1 -/-* DT40 cells immunostained with anti-Tom20 antibody. Mitochondria were fragmented in *DJ-1 -/-* cells. B. Quantification of mitochondrial size. Randomly obtained images from anti-Tom20-stained DT40 cells were analyzed by Spot Detector Version 3.0 BioApplication. The average size of Tom20-positive spots was significantly smaller in *DJ-1 -/-* cells. Error bars indicate mean ± SEM values. *P<0.05 by unpaired *t*-test. C. Quantification of mitochondrial number. The number of Tom20-positive spots per cell was significantly larger in DJ-1 -/- cells. Error bars indicate mean ± SEM values. *P<0.05 by unpaired *t*-test.

Figure 1

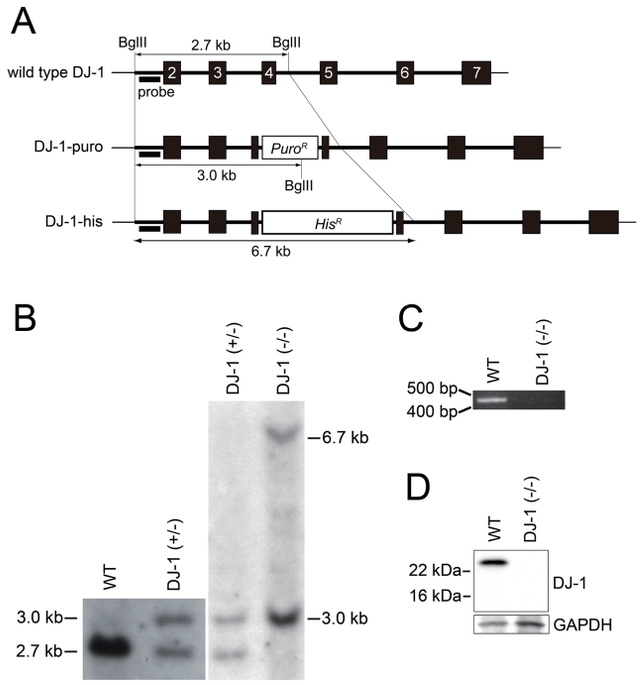

Figure 2

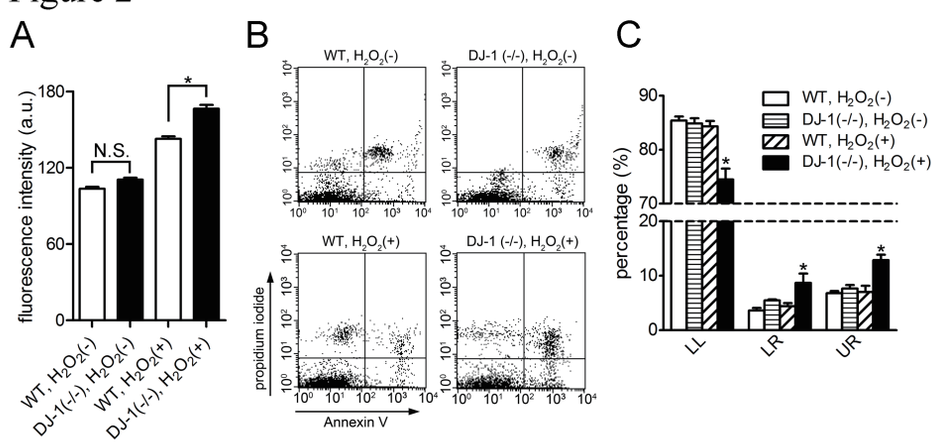

Figure 3

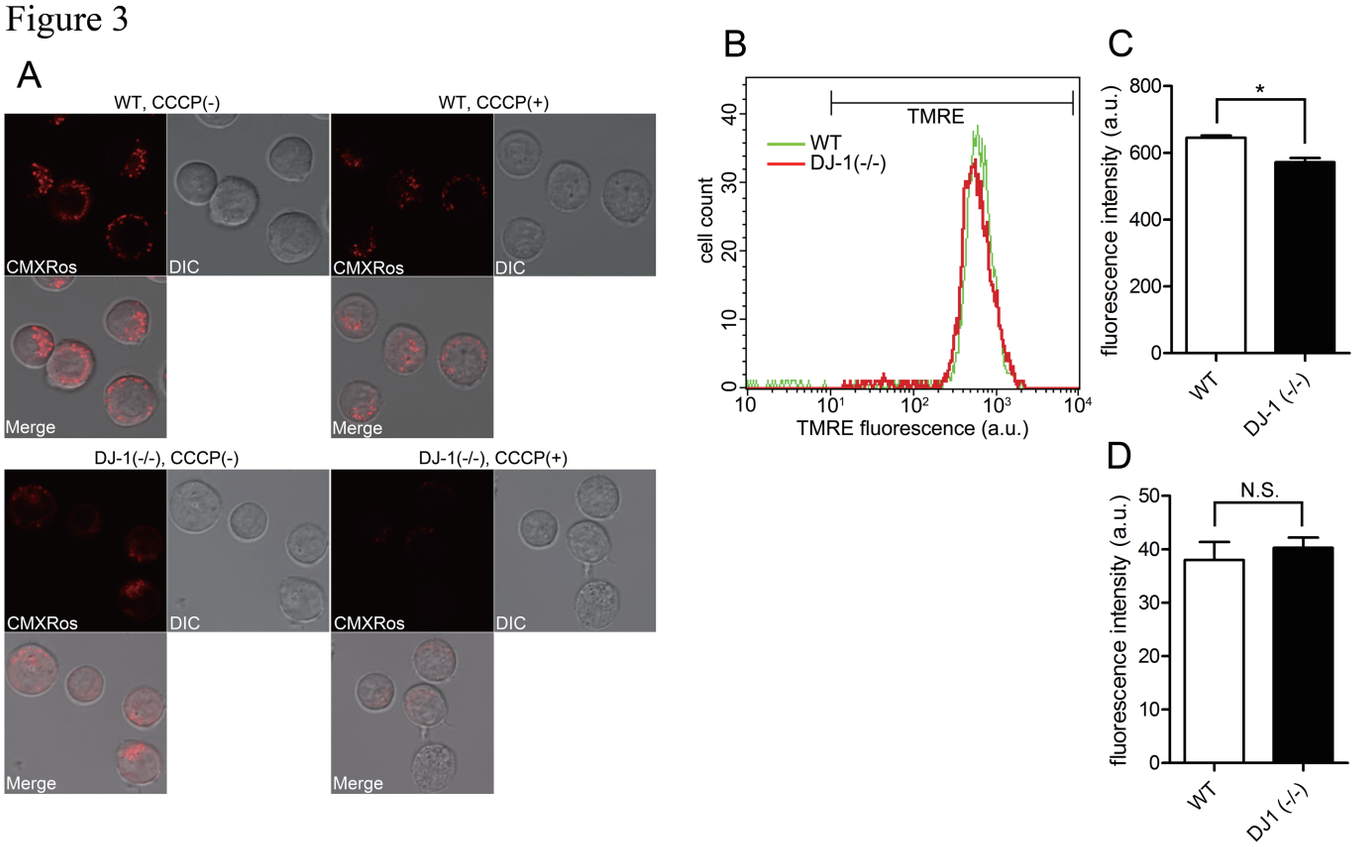

Figure 4

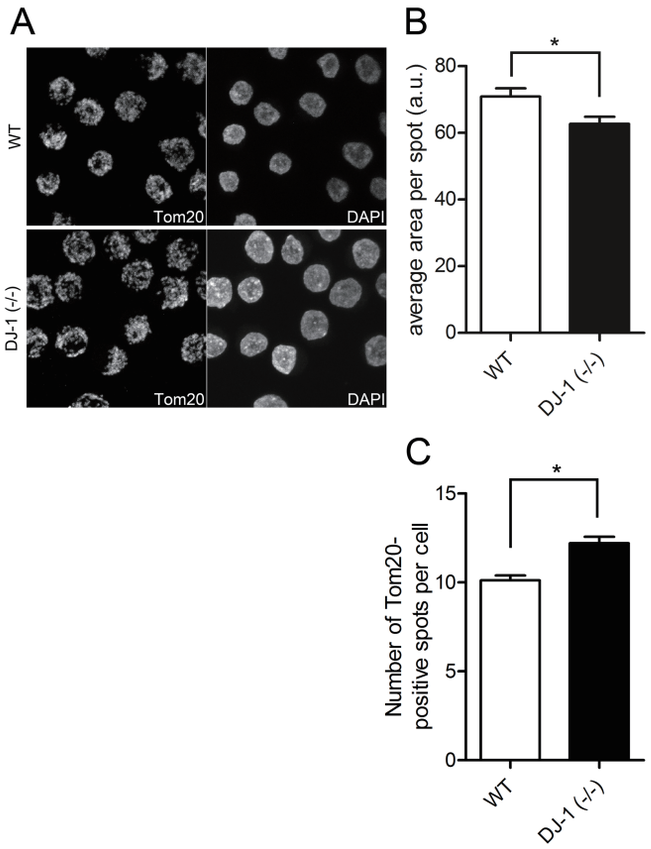
A
WT
DJ-1 (-/-)
Tom20
DAPI
Tom20
DAPI
B
average area per spot (a.u.)
80
60
40
20
0
*
WT
DJ-1 (-/-)
C
Number of Tom20-positive spots per cell
15
10
5
0
*
WT
DJ-1 (-/-)